General Disclaimer

One or more of the Following Statements may affect this Document

- This document has been reproduced from the best copy furnished by the organizational source. It is being released in the interest of making available as much information as possible.

- This document may contain data, which exceeds the sheet parameters. It was furnished in this condition by the organizational source and is the best copy available.

- This document may contain tone-on-tone or color graphs, charts and/or pictures, which have been reproduced in black and white.

- This document is paginated as submitted by the original source.

- Portions of this document are not fully legible due to the historical nature of some of the material. However, it is the best reproduction available from the original submission.

DEVELOPMENT OF A HIGH EFFICIENCY THIN SILICON SOLAR CELL

JPL Contract No. 953862

March, 1975

Final Report

Report No. SX/104/F

by

Joseph Lindmayer, et al

SOLAREX CORPORATION
1335 Piccard Drive
Rockville, MD 20850

This work was performed for the Jet Propulsion Laboratory, California Institute of Technology, sponsored by the National Aeronautics and Space Administration under Contract NAS7-100.

JET PROPULSION LABORATORY *California Institute of Technology • 4800 Oak Grove Drive, Pasadena, California 91103*

29 October 1975

NASA Scientific and Technical
Information Facility
P. O. Box 8757
Baltimore-Washington International Airport
Baltimore, Maryland 21240

Attention: Acquisitions Branch

Gentlemen:

Enclosed for your systems input and listing in the unlimited, unclassified category of STAR, are two copies of the following subcontractor reports:

953691 Xerox Electro-Optical Systems - Final Report, April 1975

953807 Pennsylvania State University - Final Report, September 1974

953842 State University of N.Y. - Final Report, 2/1-10/1/74

953846 Owens-Illinois, Inc. - Final Report, November 27, 1974

953857 Stanford University - Tech. Report No. 248, January 10, 1975

953862 Solarex Corporation - Final Report, March 1975

954082 Lockheed Missiles & Space Co. - Final Report, January 20, 1975

954155 University of Denver Research Institute - Report 180-52-02, March 1975

Very truly yours,

George A. Mitchell, Supervisor
Document Review Group
Technical Information and
Documentation Division

GAM:gb

Enclosures

Telephone 354-4321 *Telex 675421* *Twx 910-588-3294*

TECHNICAL CONTENT STATEMENT

This report contains information prepared by Solarex Corporation under JPL subcontract. Its content is not necessarily endorsed by the Jet Propulsion Laboratory, California Institute of Technology, or the National Aeronautics and Space Administration.

I. ABSTRACT

Progress during this contractual effort can be characterized by continuous improvements in all parameters of this new space cell. The Chevron^{R} metallization pattern is efficient in collecting the current and a special titanium-silver metallization provides high reliability contacts. The cells made during this effort primarily employed evaporated tantalum oxide anti-reflection coatings, which can now be applied quite reproducibly. The cells display extremely sharp I-V characteristic and high photovoltages. The blue response has also been improved significantly. In general, the efficiencies have been gradually improved throughout the contractual period.

This project has demonstrated a high-performance space solar cell having a new technological basis. Additional performance could also very likely be achieved through enhancement of the red response. It appears that the new technological basis developed during this contract warrants further "fine tuning" of the processing in order to maximize the conversion efficiency and to use the present technology to its fullest potential.

II. TABLE OF CONTENTS

III. SUMMARY

The aim of this contractual effort was to realize higher specific power output and radiation resistance from thinner silicon solar cells for space applications. The work reported herein describes the efforts applied to establishing the technological base for fabricating high efficiency thin solar cells.

The efforts expended in this project have been divided into some nine categories in the development of this new space cell. These cells are n^+-p-p^+ in form and the front n^+-p junction formation has employed phosphorus as the dopant from a gaseous PH_3 source. The p^+-p high-low junction on the back has been fabricated by alloy/diffusion of an aluminum layer applied by vacuum evaporation, which requires further study to optimize recombination site densities and enhance the red response. Cells have been processed with a starting resistivity range of 0.2-3 ohm-cm, but the low-resistivity cells require further effort to achieve reproducible surface properties. Crystal orientations employed have been (100) and (111), with the former producing less fill-factor scatter. Anti-reflection coatings for improving optical coupling of the incident light have mostly been evaporated tantalum oxide, with some titanium dioxide and yttrium oxide experimental coatings. Cells were successfully fabricated from silicon of various

thicknesses, from 15 mils down to 4 mils. Comparison of thin 4 mil cells with 10 mil cells made by the same process showed resultant power and current reduction of only 17% for thickness reduction by a factor of 2.5. Assessment of processing rate limitations for very thin silicon cells reaffirms our initial expectation that manual transfer steps presently require more care to avoid breakage, and improvements in technique have been considered. In general, the process developed in this program is amenable to very high production rates.

Calculations of theoretical limitations on cell photovoltage have been performed, including effects from distributions of photogenerated carriers. In addition, for analytical support on these efforts, modifications and improvements to optical and electronic measurement instrumentation and mathematical analysis aids have been made.

IV. TECHNICAL DISCUSSION

A. Front Reflection

The conventional way of reducing the surface reflection of light incident on silicon is to employ a quarter-wave anti-reflection coating. Traditionally, the materials employed in the solar cell industry were SiO_x and later TiO_x; but more recently, tantalum oxide has gained popularity. A single A-R coating with a refractive index greater than 2 can eliminate most of the surface reflection, and approximately 92-94% interface transmission can be achieved. The remaining reflection can be eliminated or minimized either by a graded index coating or by texturing of the silicon surface, which leads to some light trapping.

This effort has examined evaporated tantalum pentoxide for its properties in terms of absorption and refractive index. It was observed that the resulting refractive index and short-wavelength absorption are both very dependent on the evaporation conditions. One major parameter appears to be the vacuum system pressure during evaporation. Figure 1 shows R+T (reflection plus transmission) measurements for two different evaporation pressures. Tantalum oxide evaporated at low pressures, with a subsequent anneal at about 430°C results in an excellent UV window. It was noted, however, that it is harder to maintain a high index of refraction. Figure 2 shows a measurement of a sample which was obtained by

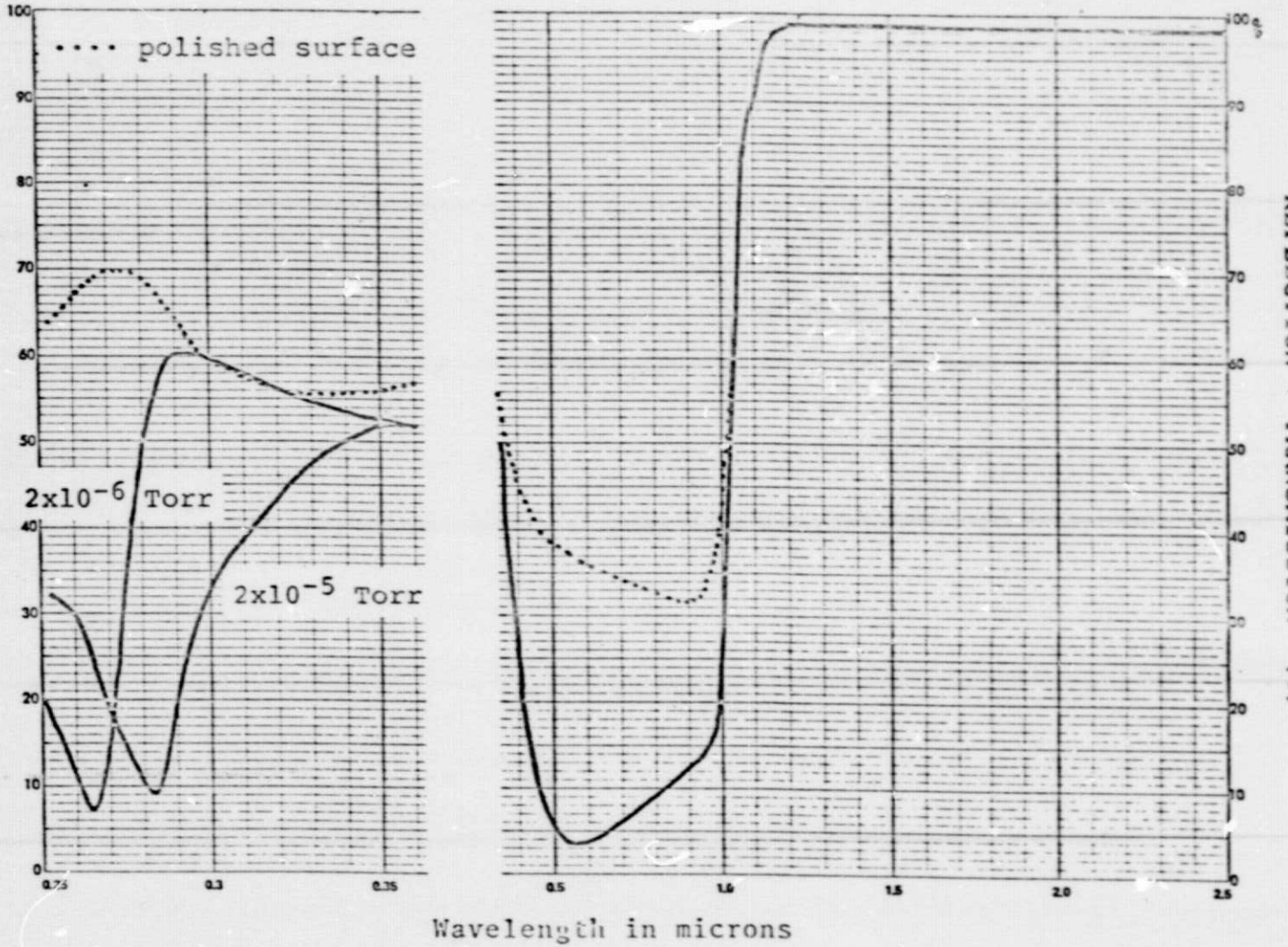

Fig. 1. Reflection + Transmission (R+T) vs. wavelength for tantalum oxide on silicon. Evaporated at 2 x 10^{-5} Torr and 2 x 10^{-6} Torr.

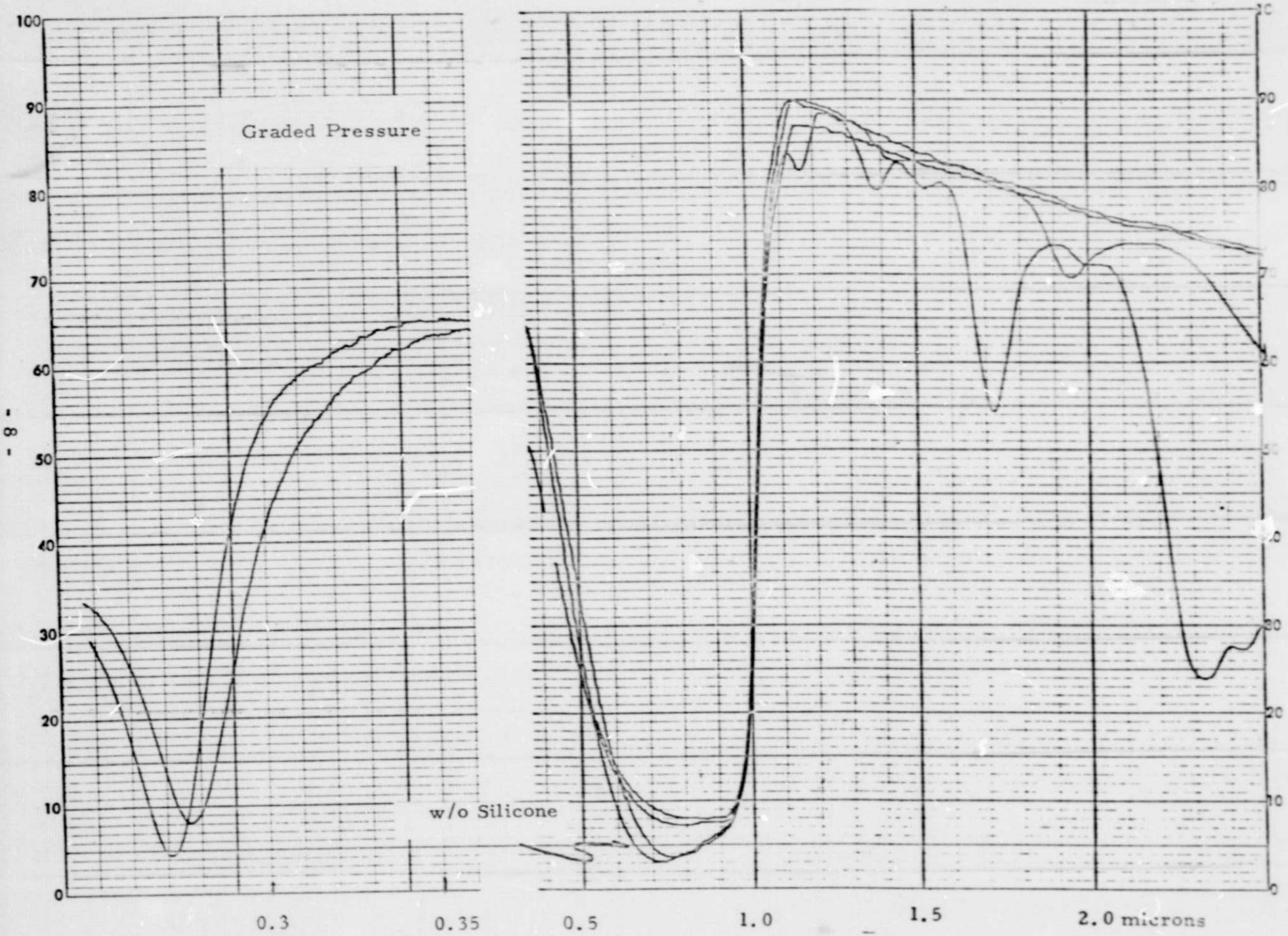

Fig. 2. Reflection plus transmission as a function of wavelength for tantalum oxide on silicon. Begun with oxygen back pressure; finished at 2×10^{-6} Torr.

varying the pressure during evaporation. A back pressure of O_2 was added in an attempt to hold stoichiometry at the beginning of the evaporation, while the final layer was deposited at low pressure. The results were somewhat inconsistent and produced no significant improvement. However, a sufficiently high index of refraction was developed by evaporating at a high rate at the lowest possible pressure. This anti-reflection coating appears to be under good control and has been applied routinely. Figure 3 shows a reflection vs. wavelength plot of a representative tantalum oxide coated cell having a high index of refraction, which produces a net drop in reflection upon application of the intermediate-index cover.

Short experimental excursions were made in the direction of employing yttrium oxide as an alternate anti-reflection coating. This oxide appears to have most of the desired properties and also shows changes in the index of refraction related to the evaporation conditions. Figure 4 shows a typical reflection + transmission curve obtainable by the application of yttrium oxide. Work in this direction was stopped, however, as the scope of this effort does not allow the full exploration of this oxide.

Another search for a better optical match consisted of the application of double layers. In particular, we employed a thin layer of titanium metal coated with evaporated tantalum oxide. Upon heating in air, in the neighborhood of 500 °C, the titanium

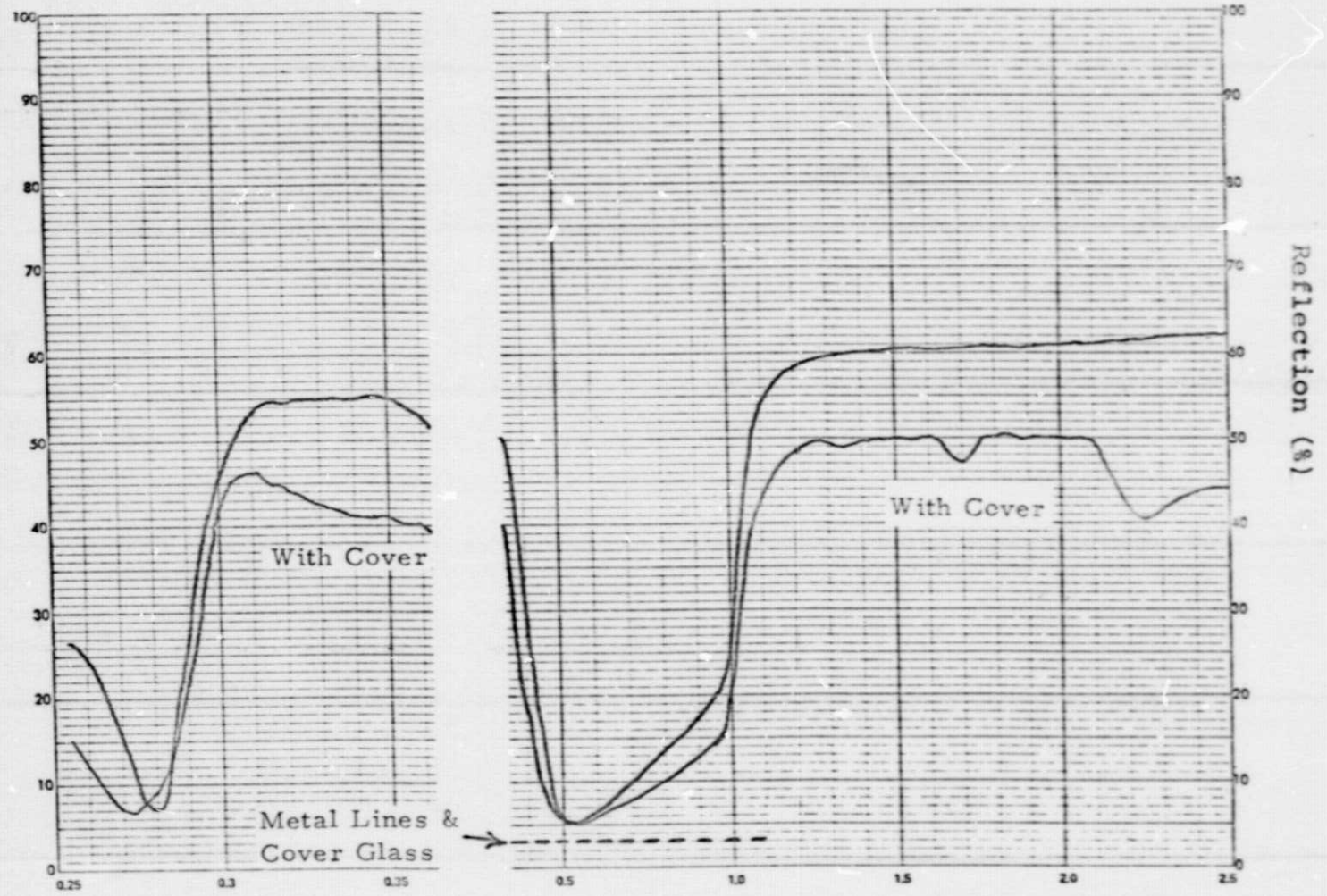

Fig. 3. Reflection as a function of wavelength for tantalum oxide deposited rapidly at low pressure.

Figure 4. Reflection plus transmission of yttrium oxide on silicon.

layer became oxidized to form TiO_2. It was discovered, however, that titanium has peculiar oxidation properties in that the oxidation rate is a strong function of evaporation condition history. Nevertheless, successful double layers were applied and an improvement in the optical match was observed following addition of a cover slide. This is shown in Figure 5. The observed passband widening of the optical transmission is due to the higher index displayed by the underlying TiO_2 layer. Again, detailed mapping of this system was terminated because of effort limitations.

B. Front Junction Formation

Diffusion of the front junction employed a gaseous source consisting of a mixture of N_2, Ar, O_2, and PH_3. The main variables controlling the diffusion process are the temperature of diffusion, the time at temperature and the gas mixture composition. The desired results are an optimum sheet resistance in the n^+ layer and minimum damage to the silicon crystal lattice. The sheet resistances obtained are quite reproducible, as determined by four-probe measurement, and are set at approximately 100 ohms per square. The degree of lattice damage associated with the diffusion process was evaluated by measurement of the dark forward current characteristics and the forward injection storage capacitance at low current densities, as described later in this report. During the effort on variation of diffusion parameters,

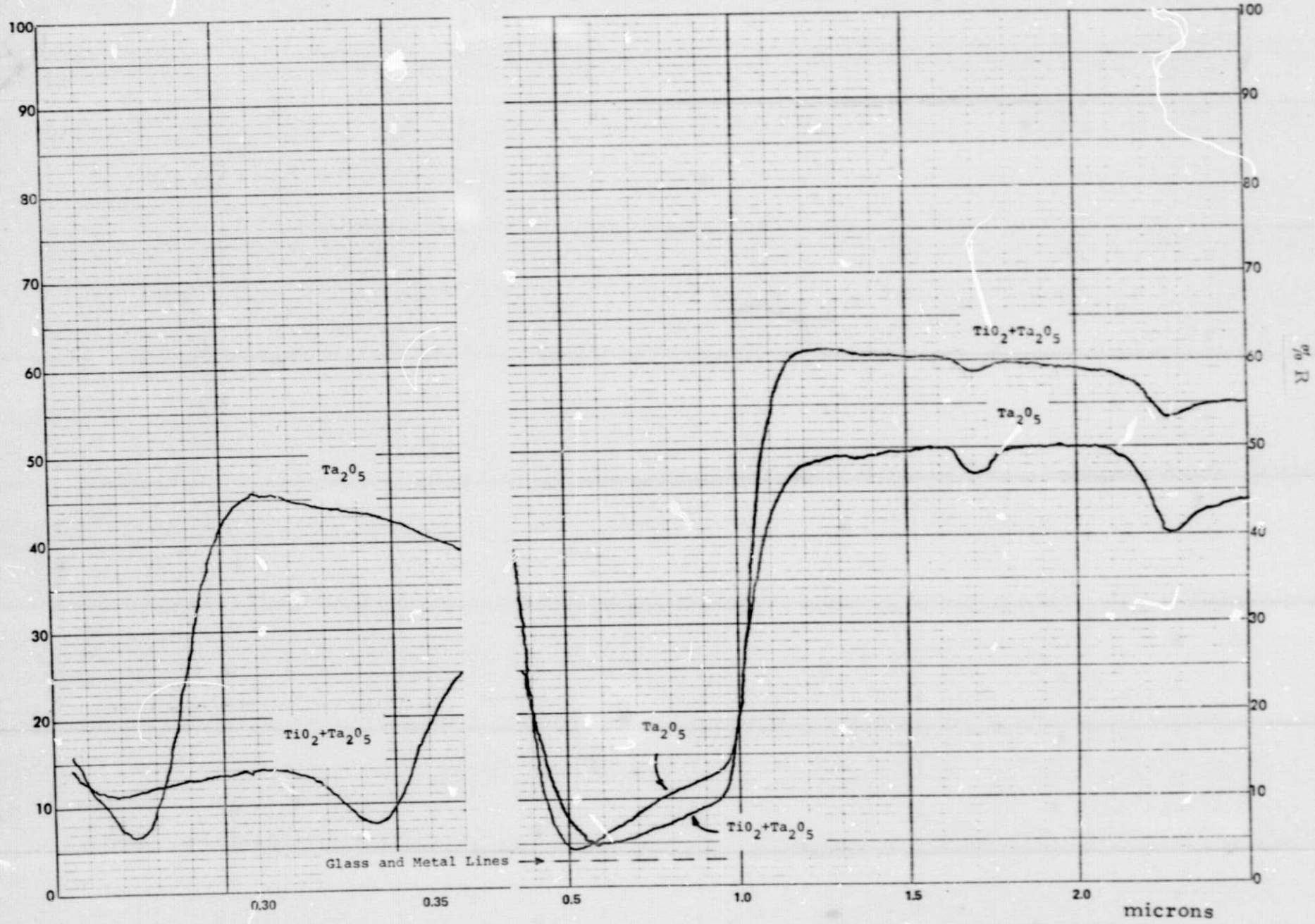

Fig. 5. Reflection of layered titanium oxide and tantalum oxide on a silicon solar cell.

it became apparent that good fill factors, improved storage times and improved dark current characteristics were obtained with diffusions performed in the neighborhood of 860°C for 10 minutes, with gas compositions near 1:10:100:100 for PH_3:O_2:Ar:N_2. These diffusion conditions have produced approximately 5mA per cm^2 of short wavelength response below 0.55 micron, using a Corning 9788 glass filter in the AM0 simulator path, as shown in Figure 6 for a 10 mil thick cell.

C. Back High-Low Junction Formation

The system investigated in this effort for forming a high-low junction at the rear surface of the cells was the diffusion/alloying of aluminum. In most cases, the aluminum was applied by evaporation and alloyed through the rear phosphorus junction. The aluminum-silicon eutectic temperature is known to be at 577°C, while considerable aluminum penetration is well known to occur down to around 450°C. At higher temperatures, the aluminum easily penetrates and overwhelms the pre-existing n^+-p phosphorus-doped junction. Above 660°C the aluminum itself goes into the liquidus phase and the whole sandwich of back layers re-solidifies on cooling. The properties of the high-low junction are then determined by the net stress and doping near the former eutectic interface and the associated diffusion front. The interfacial recombination velocity resulting from this structure

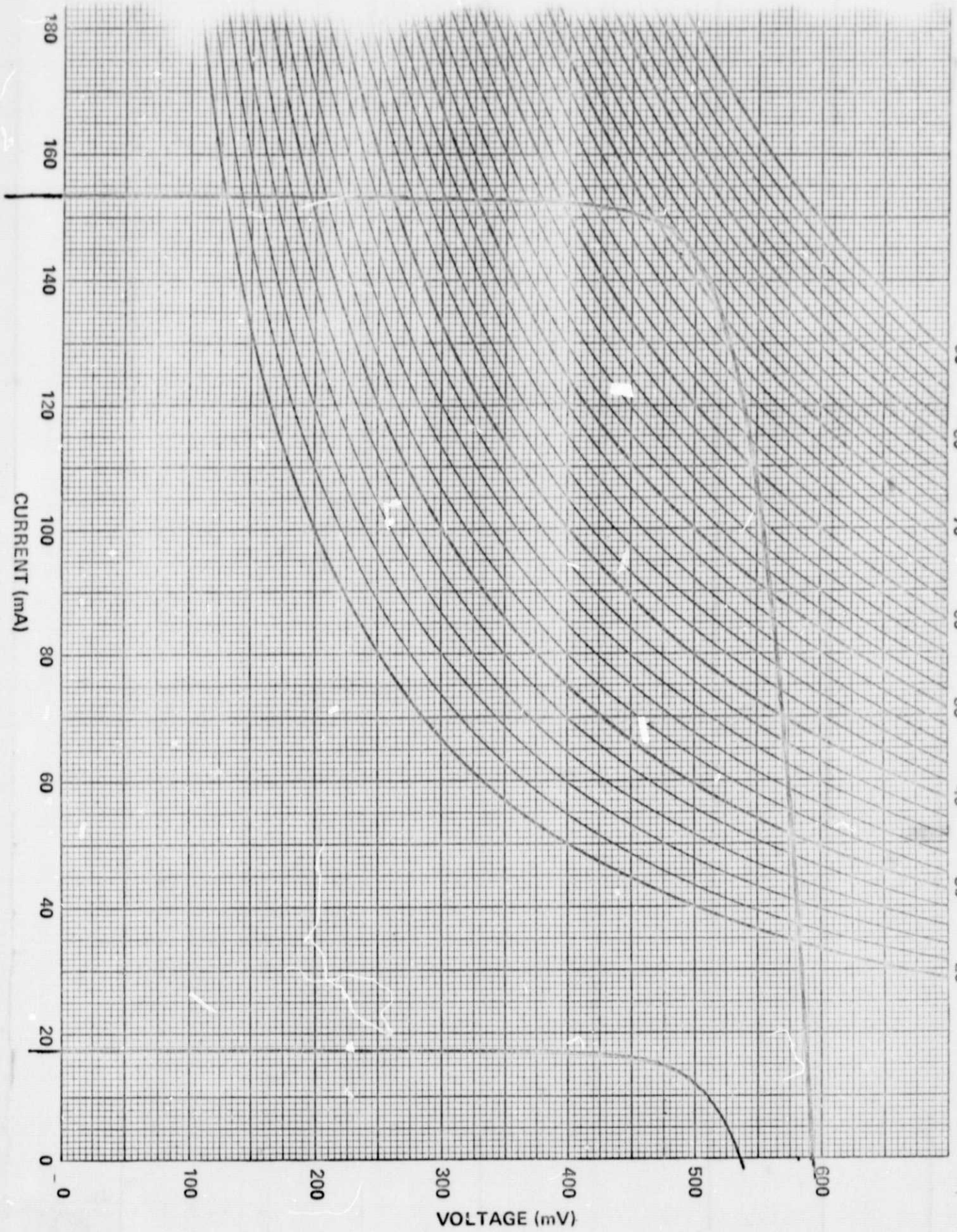

Figure 6. AM0 photoresponse of a typical 10 mil cell, with an additional curve of blue response for filtering with 5 mm of Corning 9788 glass.

determines the efficiency of reflecting photogenerated electrons toward the front junction for collection. It must be considered that too mild an aluminum penetration would leave an n^+ potential minimum which would force electron motion toward the back surface, but this effect appears to be easily overcome as shown by the data on ischronal (15 min.) alloying temperature experimentation in Figure 7. Higher temperatures of alloying appear to degrade the interfacial recombination velocity, as evidenced by the monotonic decrease in collected current with increasing temperature. However, consistently high photovoltages and the asymptotic increase in collected photocurrent with decreasing alloying temperature down to 650°C indicate no problem in overcoming the prior n^+ layer.

The resultant recombination velocity appears to be higher than hoped and a function of detailed metallurgy, as shown by the scatter in long wavelength yield in Figure 8. (The measurement technique is described in a later section). Concerted efforts were directed to improvement of carrier lifetime at the back interface, but it is obvious that this system will require further investigation.

D. Internal Reflection

We have examined some metals for rear surface application to produce a second pass of unabsorbed light. This could be an important contribution to the efficiency of very thin cells. Figure 9 shows the spectra of reflections for aluminum, titanium and chromium

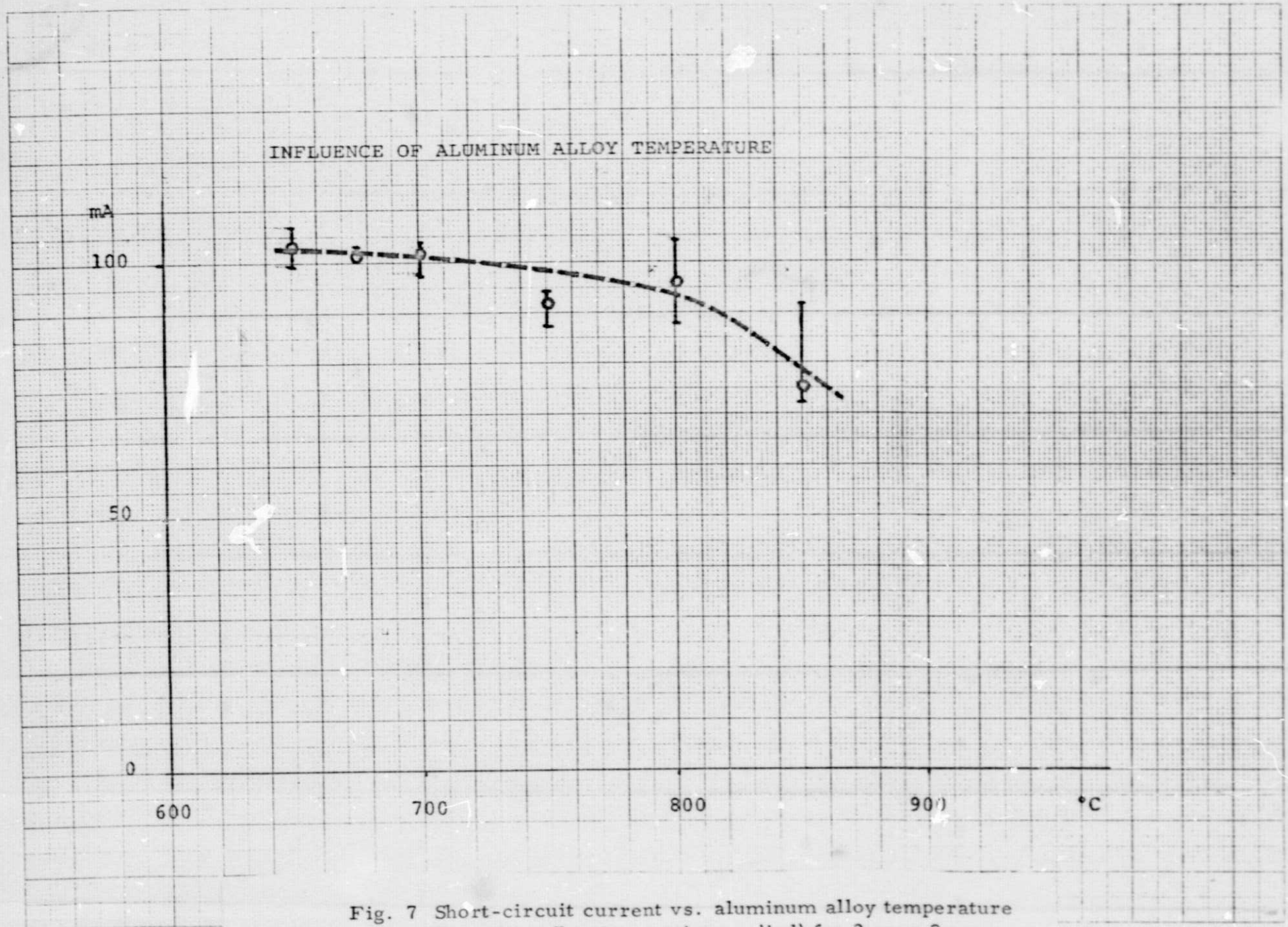

Fig. 7 Short-circuit current vs. aluminum alloy temperature (no anti-reflection coating applied) for 2 cm x 2 cm cells with 15 minute alloy.

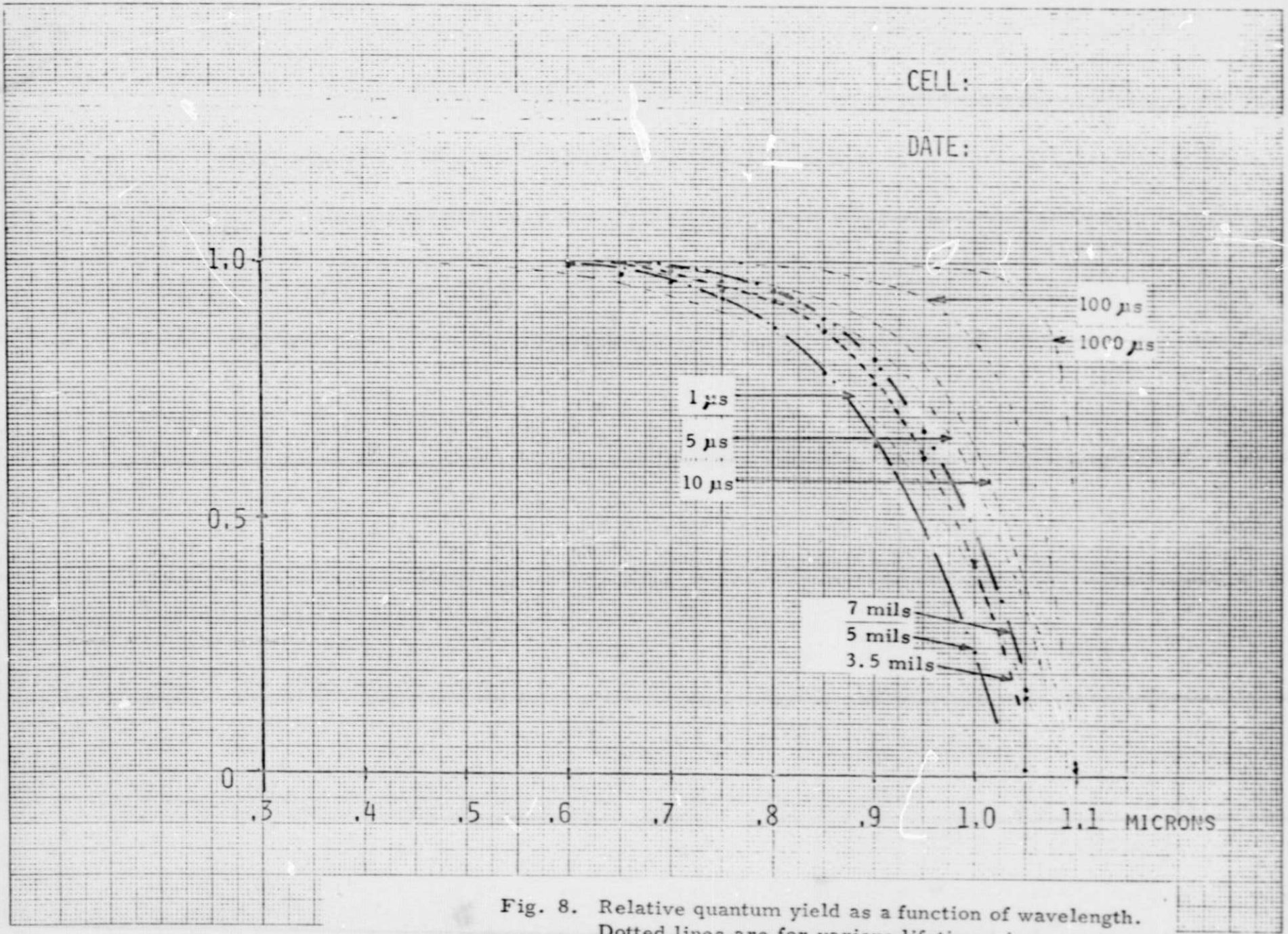

Fig. 8. Relative quantum yield as a function of wavelength. Dotted lines are for various lifetimes in a semi-infinite volume.

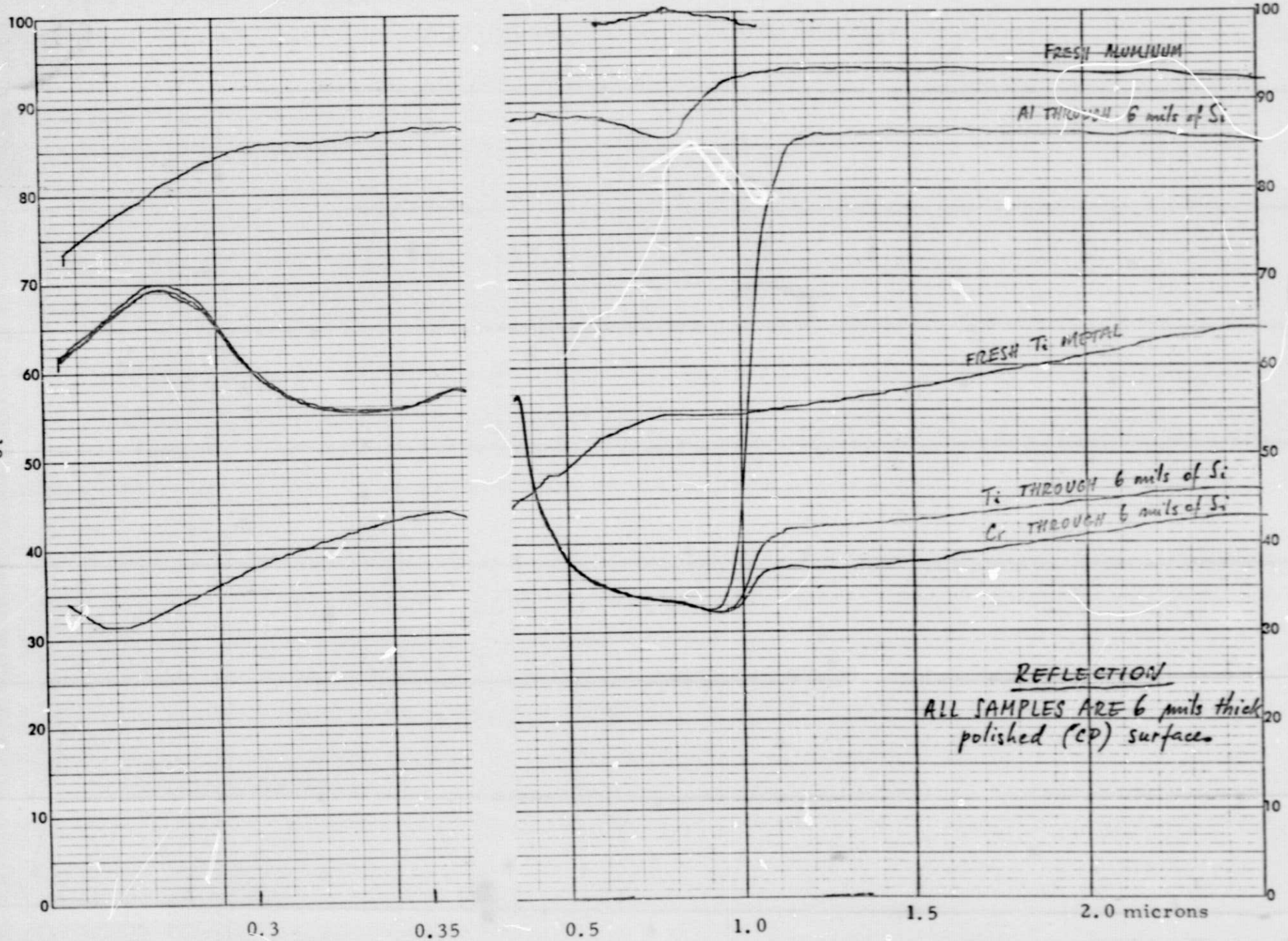

Fig. 9. Front-surface and rear-surface mirror layers on silicon.

behind 6 mils of silicon. As is apparent and expected, aluminum is a superior internal mirror. This is true as long as the metal is freshly evaporated. Figure 10 shows the degradation of the internal reflection resulting from aluminum alloying at 640°C and 700°C. This behavior of the aluminum should be examined further since aluminum is also useful for creating a p^+-p junction on the rear surface. In addition, we believe that spectral details of reflection from the silicon-alloy interface may be very useful in assessing properties of the alloy in future efforts. Note in Figure 10, however, that the alloyed interface still reflects over 60% of the light reaching the interface. This is a significant contribution to second-pass absorption capability in thin cells.

E. Crystal Orientation

In the course of the first two quarters of this effort, wafers of both (100) and (111) surface orientation were employed for solar cell fabrication. In general, the characteristics of cells having the two different surface orientations are remarkably similar, with one exception. The cells fabricated on (100) surfaces were quite reproducible in fill factor, while those employing the (111) orientation scattered quite randomly in fill factor. Devices of equal quality can be made with either orientation, but the yield for the (111) orientation has been consistently lower in our experience. Whether this effect is due to the edge orientation differences or variations in alloy or diffusion was not determined during this effort.

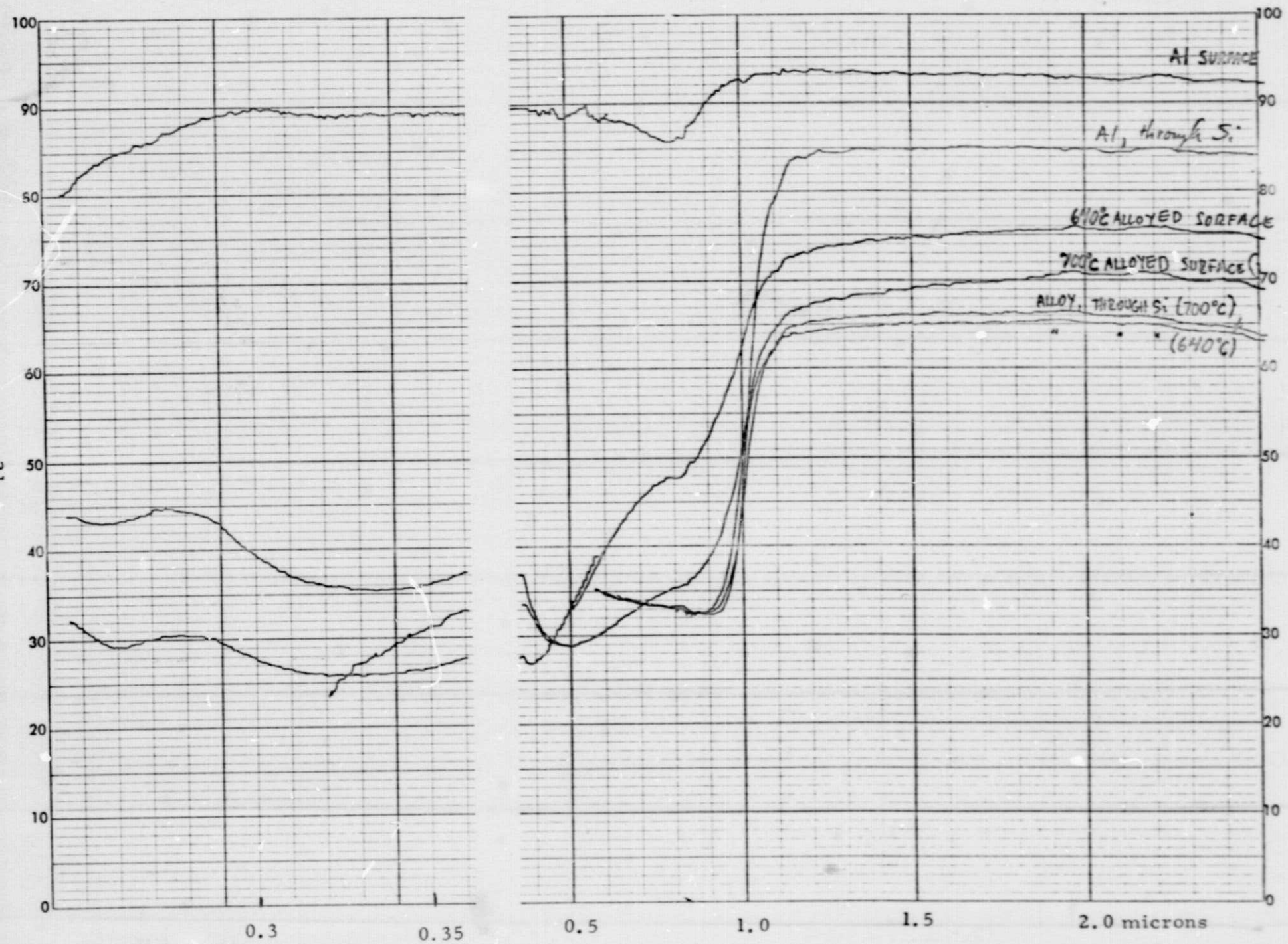

Fig. 10. Reduction of aluminum reflection with alloying.

F. Low Resistivity Silicon

A supply of p-type wafers of 0.2 ohm-cm resistivity was obtained for use in this effort. Cells were fabricated in much the same fashion as for the 2-3 ohm-cm wafers normally employed. Cell performance was fairly similar except for one outstanding aspect, the variation and instability of both the fill factor and photovoltage. This is explained by the decreasing ratio of n^+ to p doping levels, which in combination with very shallow junctions allows increasing interaction of the surface of the n^+ layer with the minority carrier distributions in the neighborhood of the junction. As a consequence, chemical interactions with the ambient, which change the surface state properties and surface potential, exert increased control over the current-voltage characteristics of the junction. The net result is that the immediate chemical history of the cell surface affects the characteristics of the cell, as can be seen in the dark-current plot in Figure 11. Control of these properties and stabilization of the fill factor for low-resistivity cells represents a level of effort which did not fit within the resources of the contract funding. Thermal oxidation techniques are well known for stabilizing surface state conditions on silicon, but the oxidation temperatures and resultant oxide thicknesses commonly employed are incompatible with low-temperature cell processing and efficient (high-index) anti-reflection coatings.

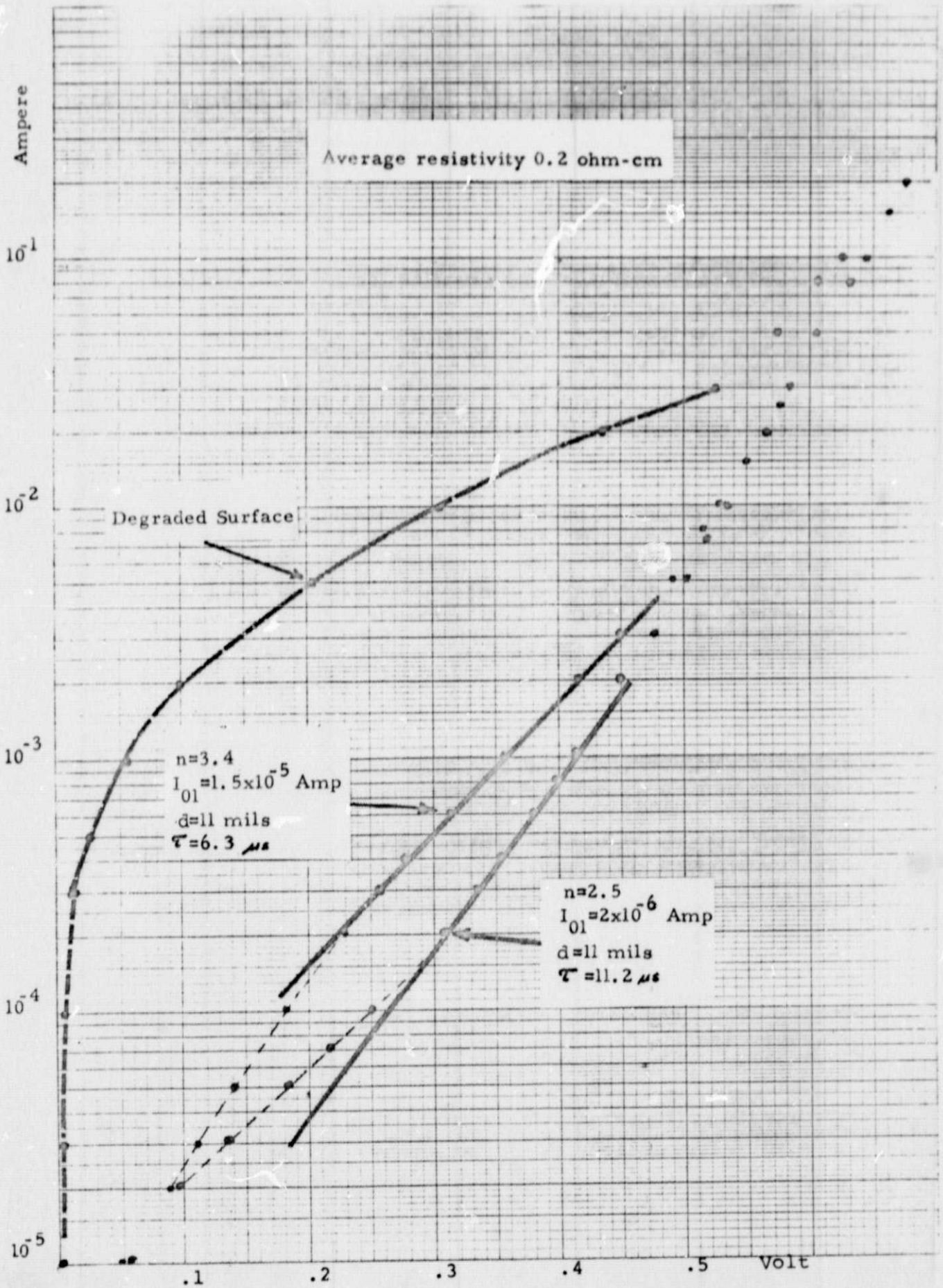

Figure 11. Range of dark I-V characteristics observed for 0.2 ohm-cm starting resistivity.

Certainly, there must be a compromise technology for achieving stable low surface state densities on low resistivity cells in conjunction with high-index anti-reflection coatings. We could pursue this subject to successful conclusion in some future efforts.

G. Thin Cells

Groups of experimental 2 cm x 2 cm cells were fabricated in silicon of various thicknesses, utilizing the best-case combination of the processing techniques described above. The silicon thickness was varied in approximately one mil steps from 11 mils down to 4 mils, employing 2 to 3 ohm-cm (100) surface orientation silicon starting material. The resulting AM0 cell performance of the groups of devices fabricated is shown in Figure 12 and Figure 13 along with data for similarly processed 15 mil cells.

These cells had tantalum oxide anti-reflection coatings at the AM0 measurement step, but no cover glass, the application of which raises the output about 5%. As expected, the short-circuit current is a slow function of thickness; losing only the long-wavelength photocurrent which would have been generated in the deep bulk as the thickness is decreased. The peak power curve undergoes the same relative drop as the current, since these devices all have excellent fill factors and the drop in open-circuit photovoltage with decreasing cell thickness was very small (varying only with the logarithm of the current). Reducing the cell thickness by a factor of 2.5 from the common 10 mil starting material only

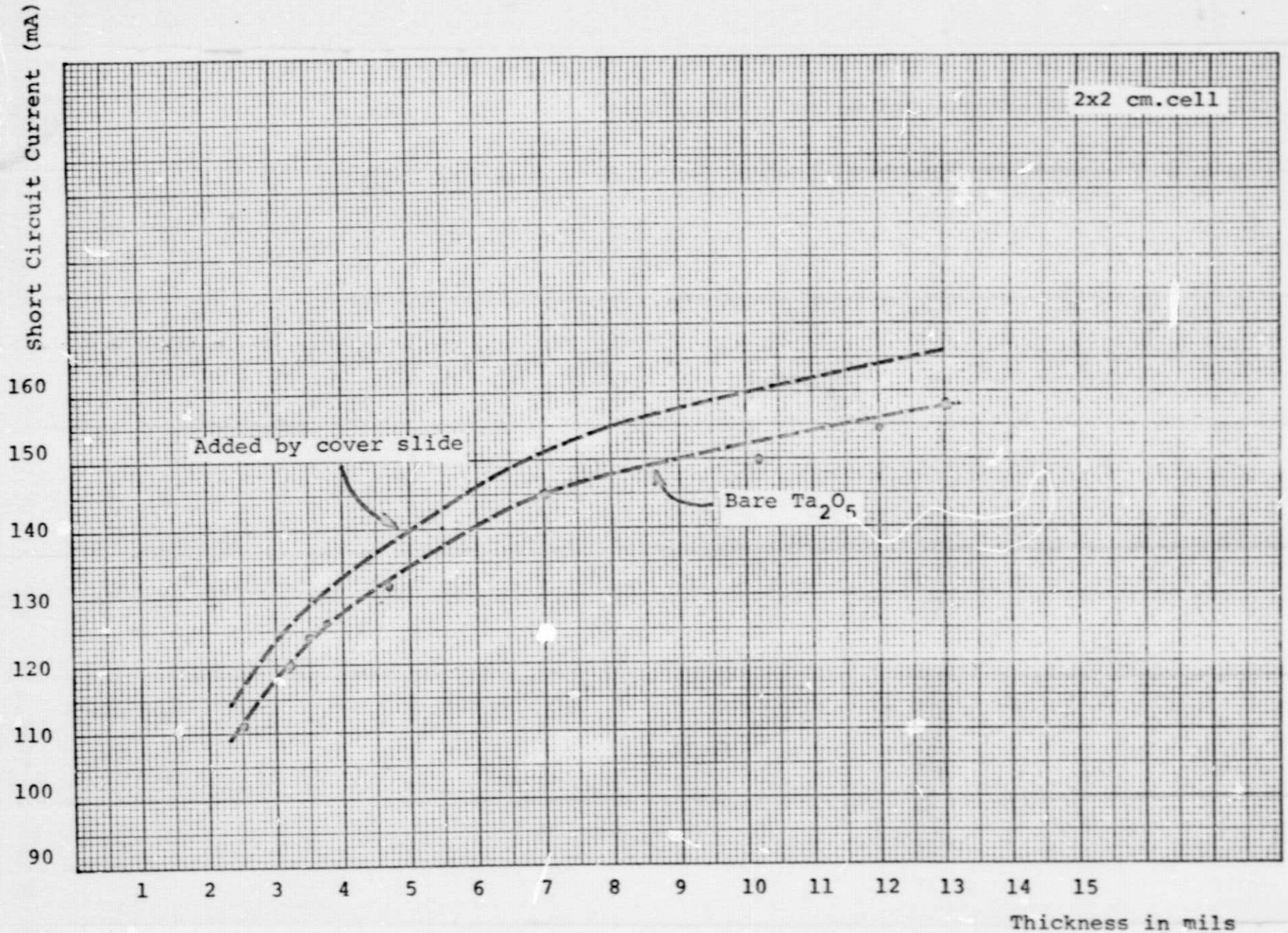

Fig. 12. Present status of short-circuit current vs. cell thickness for 2-3 ohm-cm cells.

Fig. 13. Present status of maximum power vs. cell thickness for 2-3 ohm-cm cells.

reduces the AM0 output current by 17%, a significant improvement in power to weight ratio over conventional cells.

H. Metallization Geometry

The experimental cells constructed during this effort were all 2 cm x 2 cm for convenient cell-to-cell comparison. The metallization geometry employed for current collection on the front surface was the Chevron^{R} pattern shown (at 4X) in Figure 14. It is obvious from the very sharp slope near I_{SC} in the measured I-V characteristics under AM0 illumination that no problems with series resistance were encountered in employing this grid pattern. However, calculation of the total front metal area from geometrical measurements made on the cells revealed almost 10% area coverage blocking the incident light. A first-cut redesign of the mask was performed to attempt to approach only 5% light blockage by the metallization pattern. This effort started in the last quarter of the contractual period and only the final devices utilized this finer-line pattern to improve the output current.

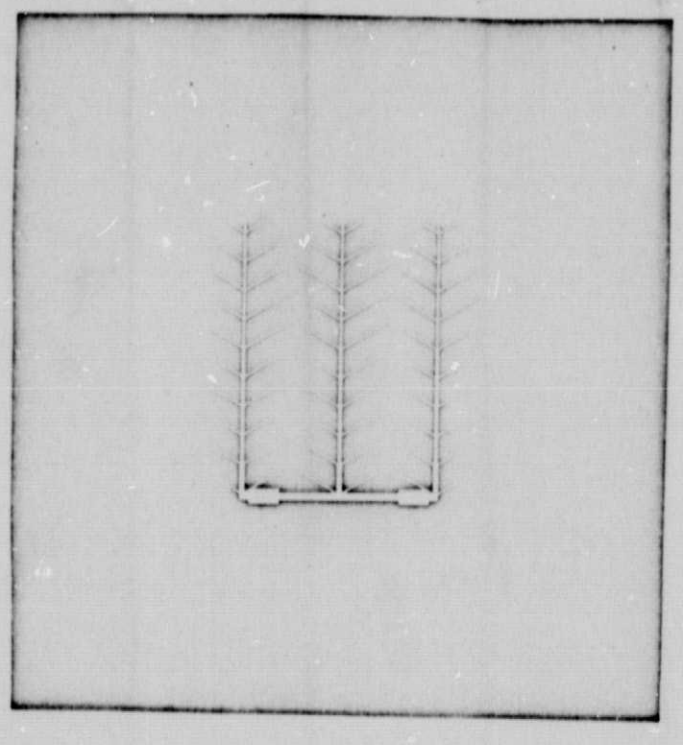

Fig. 14. Metallization pattern for 2 cm x 2 cm cells (shown 2x size).

I. Photovoltage

The photovoltage of a cell can be related to the theoretical reverse current of the junction. In a mathematical formulation of the I-V characteristics thermal generation centers must be identified. If one assumes that the bulk lifetime within the cell is relatively high, the source of the reverse current must be located at the cell's boundaries. In such a case, the reverse current components are determined by contributions to thermal generation from the appropriate surface recombination velocities. On the back side, the thermal generation centers are determined by the technology employed. While the problem of forming a high-low junction seems almost trivial, the actual technology applied to cell fabrication determines the density of thermal generation states introduced into the lattice. (This factor, of course, also relates to the red response of the cell.) At a properly diffused front junction, the surface recombination velocity is determined by the heavily doped portion of the diffused layer, mainly involving the first few hundred angstroms. When one has a junction plane that is only another couple of thousand angstroms deeper into the silicon, the reverse current component from the front layer is controlled by the surface recombination velocity. Numerical calculations show that for bulk resistivities less than 1 ohm-cm, this component is the dominant portion of the junction reverse current. The photovoltage associated with these practical limitations is approximately 600 mV at a one-sun illumination level.

It has been recognized for some time that a photovoltage contribution arises from the rear high-low junction for lightly doped substrates. However, in order to increase the photovoltage significantly above 600 mV, the details of the front junction must be better understood. Clearly, this reverse current component is a delicate function of the details of the impurity concentrations and profiles throughout the cell. Experimental excursions into this area (using 0.2 ohm-cm substrates) indicate a basic device instability. More precisely, the photovoltage and the fill factor for heavily doped substrates become a function of the precise surface treatment, such as chemical cleaning, type of AR coating, temperature treatments, etc. It appears certain now that an entirely new set of empirical parameters enter the situation. Concerted exploration into this new area has not been done in the past. Increased understanding of this problem would result in a gradually improving photovoltage with feedback to processing experimentation.

J. Processing Rate Limiting Steps

The processing technology employed for these experimental cells at Solarex is very tractable and will lend itself well to high-rate fabrication. We firmly believe that a pilot-line level of fabrication would be most useful for fine tuning of the various steps to maximize performance. The main rate limiting steps now appear to lie in

handling and cleaning of the more fragile thin silicon. No problems were encountered with thinner silicon in high-temperature steps, but rather in the manual transfer stages. The most fruitful processing rate improvement for thin cells lies in the equipment methodology for handling and holding devices. Venturi-tweezer pickups and low-force jigging for drying and evaporator mounting, would reduce the great care and time consumption presently required in these steps. The other processing steps lend themselves well to high-rate batch or continuous-flow operations with no particular precautions required for thin cells. All operations could lead to very high throughput rates, even though a fine-geometry metallization pattern presently requires photolithographic techniques similar to the steps employed in integrated circuit fabrication. This step has required hand operations, but automated machinery has been developed for very high throughput rates in the integrated circuit industry and could easily be adapted to handling thin cells.

K. Electrical Analysis Measurements

The physical properties of cells fabricated in the course of this project were analyzed by both optical and electronic techniques to determine the effects of experimental alterations of the processing technology. Measurement of photovoltaic conversion performance under calibrated AM0 conditions in the simulator does not lend sufficient insight into the operation of the various component portions

of the cells. Consequently, measurements are also performed to evaluate optical coupling efficiency at the front surface, dark-current characteristics, carrier lifetime near the front junction, and carrier lifetime near the rear high-low reflector junction. The optical coupling measurements were described above in conjunction with A-R coating evaluation and we shall discuss here the electronic analysis measurements.

1. Voltage-Current Characteristics

Dark current in a solar cell can be expressed for our purposes as:

$$I = I_{01}\left[e^{qV/nkT} - 1\right] + I_{02}\left[e^{qV/kT} - 1\right]$$

The first term of this expression represents an excess current, and the second the ideal diffusion injection. It may be assumed that the excess current is associated with thermal generation sites in the depletion region. In room-temperature silicon $I_{01} \gg I_{02}$, which means that at low voltages the first term is larger, but above a moderate voltage the more rapidly rising second term becomes dominant.

I_{01} and n indicate the deviation of a given specimen from an ideal diode, and their measurement allows assessment of the lattice damage asso ated with front junction formation. The values of n, I_{01} and I_{02} were determined from the slopes and intercepts of the dark log I vs V characteristics for silicon cells having different

resistivities and thicknesses. Figure 15 shows some of the dark I-V characteristics for 2 ohm-cm cells of thickness 4, 5, and 7 mils, while dark current plots for 0.2 ohm-cm cells having thicknesses of 10-12 mils were shown in Figure 11.

It was noted that there is a logarithmic correlation between the extrapolated excess current, I_{01}, observed for any particular cell and the exponential constant, n, as shown in Figure 16. Although these two factors can be influenced by different mechanisms, it is tentatively believed that they are both increased by high defect densities at the n^+ side of the depletion layer.

2. Injection Storage Lifetime

The measured dark capacitance of a p-n junction is the sum of the depletion layer capacitance and any diffusion capacitance. The diffusion capacitance represents charge storage in the form of injected excess minority carriers in transit. The charge stored for a forward current, I, is $I \times \tau$, where τ is the lifetime of the injected minority carriers in the more lightly doped region (if the back contact is not very close to the injecting junction).

The storage capacitance of injected minority carriers introduced by forward bias was measured using a General Radio 1656 impedance bridge. For currents above 10^{-4} Ampere, the junction conductance was too high to allow accurate capacitance measurement; therefore, the capacitance was only measured up to 1×10^{-4} Amperes.

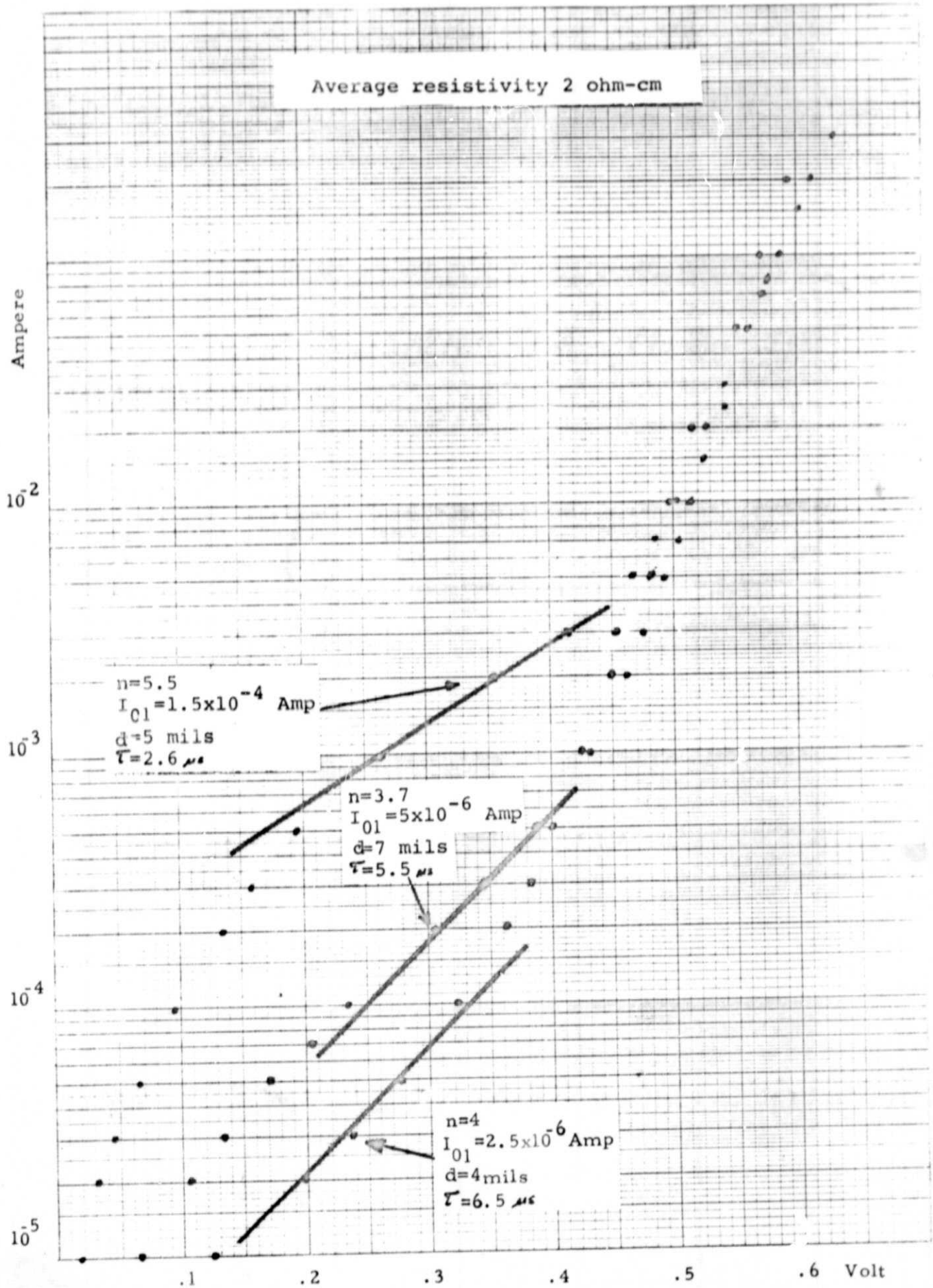

Figure 15. Representative dark I-V characteristics observed for 2-3 ohm-cm cells.

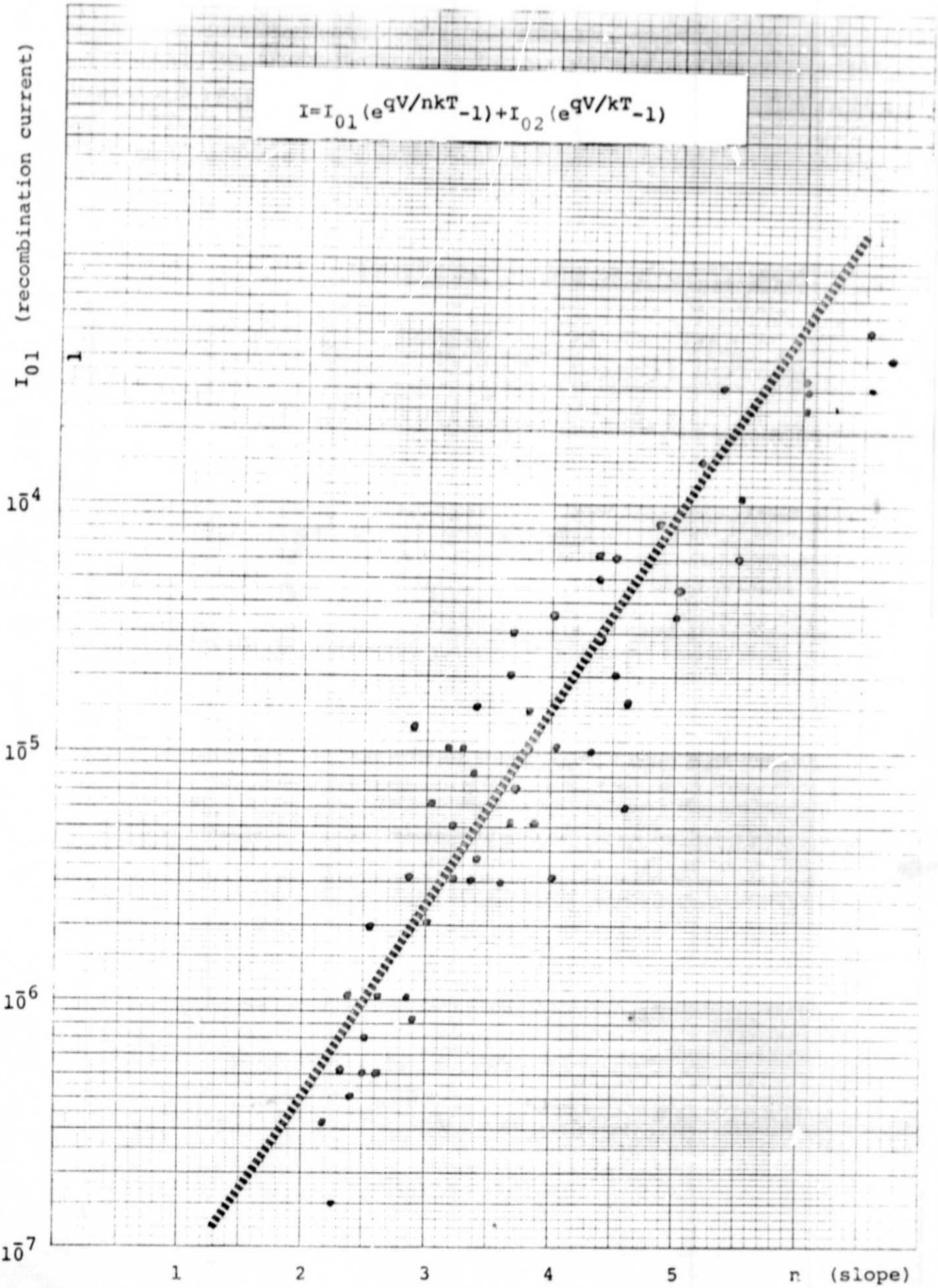

Figure 16. Correspondence of extrapolated excess current and exponent modifying factor, n, for a large quantity of cells.

From these measurements an effective carrier lifetime was calculated and since the storage capacitance was measured at low current levels where $I_{01} \gg I_{02}$, it is to be expected that the lifetime values derived apply to the front depletion layer. Therefore, the storage capacitance measurement for low current levels indicates how well the silicon crystal survived front junction fabrication. Values derived from such measurements are also indicated on the log I vs V plots in Figure 11 and Figure 15.

3. Quantum Yield and Bulk Lifetime

The basic purpose of this measurement effort was to investigate a simple method for determining the effect of the rear high-low junction formation on the effective lifetime of minority carriers generated deep in the cell.

Experimentally, the output of cells exposed to a light flux with a narrow spectrum band was used as the measurable parameter. The light flux was maintained constant as wavelength was varied and the cell output at any particular wavelength was normalized to the output observed at 0.6 micron. These values were plotted on top of a set of calculated yield versus wavelength curves derived for a semi-infinite solid. From these plots, the minority carrier lifetime could then be estimated, as in Figure 8. It is expected that the lifetime values derived apply to the deep bulk of the cell and that this measurement indicates the relative performance of back junction electron reflectors.

V. SUMMARY AND RECOMMENDATIONS

While the funding of this project was modest, it has been very instrumental in establishing a new baseline technology for space solar cells. As in any fresh start, the efficiencies were relatively low at the beginning of the effort, but continuously gradually improved throughout the contract. The net result of this project is the creation of a new thin space cell with respectable efficiencies.

From past experience, it may be said that the full potential of a new cell and the associated baseline technology cannot be developed completely in nine months. There were, however, steady improvements throughout this period and it is reasonable to expect that the efficiency would continue to increase in future efforts.

At the beginning of the project, typical efficiencies of the 2 x 2 cm cells were at conventional values, about 56mW/4cm^2. By the end of the nine month period, the efficiencies of 10 mil cells passed the 70mW/4cm^2 mark; in other words, they exceed 13% (AM0) efficiency. The improvement rate was about 1.5mW/month, which number is quite high. While this figure will decrease as the efficiency becomes higher, a significant improvement rate could be maintained for some time to come.

This investigation began by concentrating on fill factor and photovoltage problems; parameters that are related to the front side of the device. Extensive work was done in the direction of understanding diffusion conditions and, in general, the factors determining the quality of the front junction.

While these developments were being pursued, somewhat less attention was paid to the properties of the rear high-low junction, which controls the red response. It seems certain that we can maintain the photovoltage between 580-600mV and the fill factor between 78-80%. We are particularly satisfied to see these high fill factors and it is probable that this technology has produced the narrowest yield distribution of all existing technologies.

The development of a new baseline technology apparently cannot succeed without extensive experimentation. Optimization of critical cell parameters requires utilization of many disciplines, in particular, solid state physics, chemistry, and metallurgy. Due to the increased number of relevant interactions in a more sophisticated technology, a programmed technological variation may improve one of the parameters, while somewhat degrading another. Progress therefore tends to be gradual rather than occurring in discrete large-magnitude steps. As the solar cell efficiency continues to increase, the interactions among the input parameters become more delicate and the number of experiments, as well as the lot size, must be increased if one is to understand such interactions. We have used a greater number of samples during the contract than were proposed and an even larger number would be required in further development.

Now that a baseline technology is at hand, a number of parameters should be "fine-tuned". The major areas of interest are:

1) Mask Optimization

Most of the samples reported employed a metallization pattern

that covered about 10% of the frontal area. In future work the line width should be reduced and some corrections made in the line structure to minimize the blockage of incident light.

2) Diffusion Parameters

This is a very complex portion of the process, involving numerous ill-defined parameters. Temperature, gas composition, flow rate, temperature programming, inclusion of arsenic, gas programming, etc., are all important parameters requiring some statistical evaluation. While the present diffusion is carried out in the temperature range of 840-860 ^{o}C and the gas composition is defined, variations in blue and red response can still be observed which could be evaluated only on a large number of samples.

3) High-Low Junction

A detailed program for aluminum alloying including addition of other materials still requires further mapping to minimize the rear surface recombination velocity. During the formation of the rear high-low junction, the crystal lattice is easily damaged. As a result, we have to learn how to minimize damage by varying the composition of the materials, their thicknesses, temperature programs, etc. Only such experimentation can pinpoint the compositional technology that will provide the lowest possible surface recombination velocity. While all of this is happening, attention should be paid to potential adhesion problems for back contacts.

4) Handling Techniques

In order to assure high yield for thin cells in a production environment, efforts will be required along the lines suggested in this report pertaining to development of handling equipment and methodology.

Efforts in the above-mentioned areas will lead to an increasingly better defined process which could be used to manufacture cells with a predictable yield and performance. Progress in this contract was continuous and without question the efficiency could be raised yet significantly higher. We have confidence that continued effort could raise the efficiency into the range of 14-15% (AM0) at 10 mils and correspondingly higher for thin cells.